Ulrich E. Klotz * and Dario Tiberto
fem – Research Institute for Precious Metals & Metals Chemistry
Schwaebisch Gmuend, Germany

** corresponding author:*
Tel. +49 7171 1006-700
Fax +49 7171 1006-900
E-mail: klotz@fem-online,de

Dr. **Ulrich E. Klotz** is Diploma Engineer in Physical Metallurgy (University of Stuttgart, Germany) and holds a PhD in Materials Science from ETH Zurich, Switzerland. He is Head of the Department of Physical Metallurgy at the Research Institute for Precious Metals & Metals Chemistry (fem) in Schwaebisch Gmuend, Germany.

Dario Tiberto has a Bachelor of Science in Mechanical Engineering (Politecnico di Torino). He works in the Department of Physical Metallurgy at the Research Institute for Precious Metals & Metals Chemistry (fem) in Schwaebisch Gmuend, Germany.

In the past, materials have exclusively been developed by empirical correlation of chemical composition, manufacturing processes, and obtained properties. This processing, based mainly on guesswork and good luck, in the age of increasing experimental costs has been overshadowed by rapidly developing computational materials design. In many industries modern simulations tools are successfully applied for the improvement of materials and processes, while in jewellery technology their potential is only used to a limited extent. This paper describes different simulation methods and shows how these could be applied in jewellery technology in a meaningful way. Thermodynamic simulations allow the calculation of phase diagrams, which are required for alloy design, heat treatment processes and to understand segregation phenomena. In contrast to binary and ternary diagrams from handbooks the simulation allows dealing with real multicomponent alloys. Examples from higher order gold alloys will illustrate the possibilities. Computational fluid dynamics (CFD) can be used to describe the complex flow of the melt during casting and the temperature distribution as a function of time. However, rather than providing exact solutions up to the last process parameter, the CFD simulation can be seen as a tool for the improvement of casting quality, in order to establish helpful guidelines. Examples from static, tilt and centrifugal investment casting will show the possibilities and limits of the simulation. In the outlook the potential and requirements for further use of simulation techniques in jewellery technology will be discussed.

Computer Simulation in Jewellery Technology meaningful use and limitations

1 Phase diagrams and thermodynamic simulations

1.1 Principles of phase diagram simulations

Phase diagrams describe the stability ranges of different phases (gas, liquid or solid phases with different crystal structure) as a function of temperature, composition, pressure and other variables. The most frequently representation is as a function of composition and temperature. Phase diagrams are considered as roadmaps for materials design [1], because based on the knowledge of the stability ranges of different phases the material properties can be understood and improved. Typical examples are the melting range of alloys, the age-hardening response of gold alloys etc. Phase diagrams are usually comprised in handbooks of binary and ternary alloy systems [2]. For gold alloys handbooks on binary [3] and ternary systems [4] are available. However, as many modern alloys contain more than two alloying elements the knowledge of binary and ternary systems alone is not sufficient for alloy development anymore. Therefore, since the 1970ies modelling and simulation tools and databases have been developed in order to calculate higher order systems. This approach is also known as CALPHAD (Computer coupling of phase diagrams and thermochemistry) [5, 6]. Nowadays, different software packages and databases for different materials (steels, Al, Ni, Ti, Mg alloys, precious metals) are commercially available. For the calculations in this paper the software ThermoCalc® was used with the databases SNOB1 and SSOL4. In the following chapter the applications of such simulations for jewellery technology will be described.

1.2 Equilibrium calculations of binary systems

Many binary alloy systems are well investigated. The phase diagram can be plotted as a two-dimensional figure showing the stability ranges of the different phases as a function of composition and temperature. For example, Figure 1 shows the binary Ag-Cu phase diagram. It is characterised by a eutectic point (melting minimum) at about 28% Cu and 780°C. A 925 Sterling silver alloy has a melting range from 897 – 802°C and shows a single phase microstructure from 802 – 761°C before the solubility limit for Cu is reached and precipitation of a Cu-rich phase occurs. During cooling of the melt the alloy precipitates a Ag rich solid solution at the liquidus temperature. During subsequent cooling the concentrations of the melt and the solid phase shift according to the phase diagrams and the green tie-lines show the compositions in equilibrium at a certain temperature. This process requires sufficient time for the diffusion of the alloy elements (equilibrium condition).

It is important to note that all phase diagrams usually describe the equilibrium conditions of a system. In practice this equilibrium is often not achieved especially in the solid state where the diffusion rates are usually slow. In the Ag-Cu alloys this results in a segregation of Cu in the melt and as a consequence the composition of the melt follows the liquidus line until the end of the solidification. In case of 925 Sterling silver the solidification ends at the eutectic composition resulting in a two-phase microstructure. The microstructure of the as-cast condition is shown in Figure 2. The eutectic regions can be clearly identified by their lamellar structure. Furthermore, the Ag rich phase shows precipitates of the Cu rich phase, which formed during slow cooling in the solid state. After annealing at 800°C for 1h followed by water quenching the equilibrium microstructure of a single Ag rich phase is achieved.

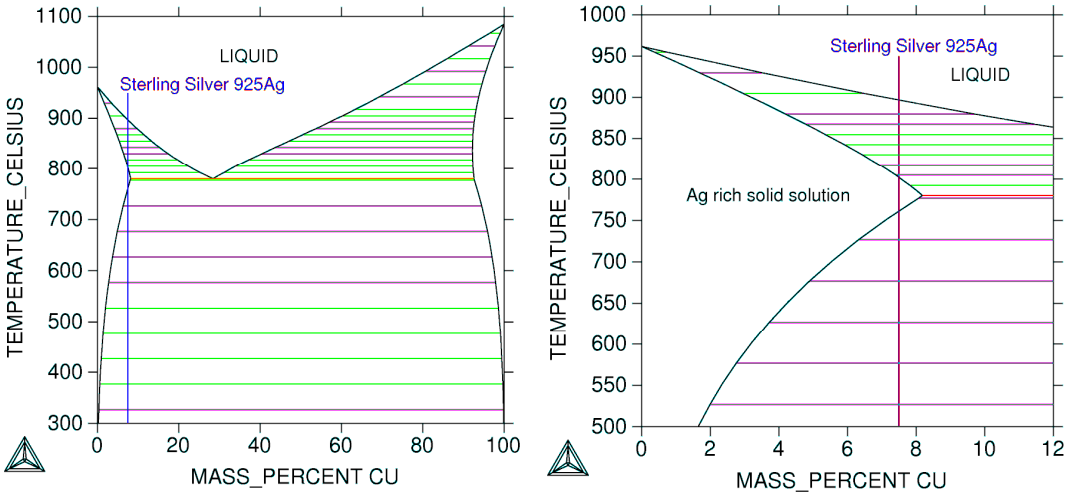

Figure 1: The binary Ag-Cu phase diagram (left) and a magnification of the silver rich side (right).

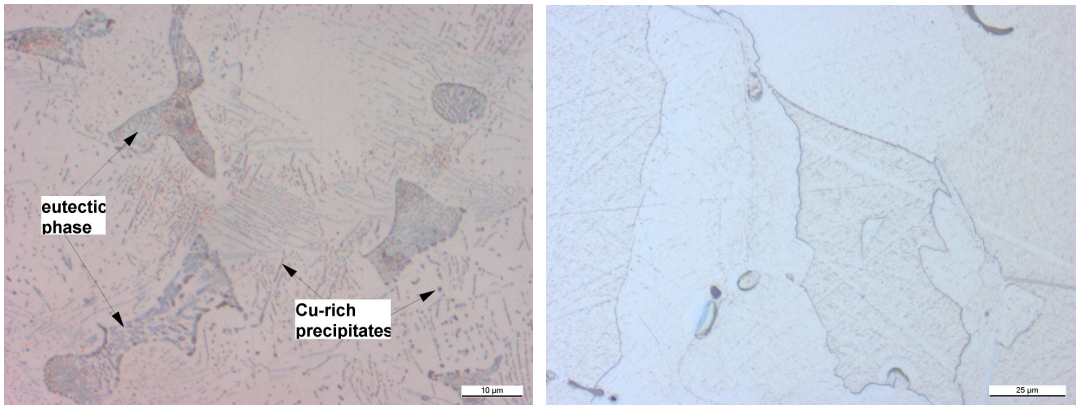

Figure 2: Microstructure of a 925 Sterling silver alloy in as cast condition (left) and after annealing at 800°C for 1h followed by water quenching (right).

1.3 Higher order silver alloys

The handbooks of phase diagrams are restricted to binary and ternary systems. Because of their complexity higher order systems are often not investigated experimentally. Nevertheless most technical alloys (e.g. steels or Ni base alloys) contain up to ten alloying elements. A thermodynamic database collects experimental information on phase diagram and thermodynamic data of binary and ternary systems. Based on this information extrapolations to systems containing more than three elements are made. However, the user always has to check for the reliability of the calculated results by comparing them with selected, reliable experimental data.

Besides copper a frequently used alloying element in 925 silver alloys is zinc. It is known to improve form filling and helps to avoid firestain [7]. Firestain is caused by internal oxidation of the Cu rich eutectic regions in Sterling silver. A section trough the ternary Ag-Cu-Zn system is presented in Figure 3. The exchange of Cu by Zn slightly reduces the liquidus temperature and narrows the melting range. For up to 2% Zn this effect is still relatively small. Zinc dissolves in silver much better than Cu does and therefore reduces the stability of the Cu rich solid solution (CuSS) and the Ag-Cu eutectic. This explains the positive role of Zn on firestain resistance.

The addition of small amounts of silicon to silver alloys has a tremendous effect on the alloy properties. Silicon is used in small amounts up to 0,2% and is known to reduce the formation of copper oxide and to improve the form filling. However, is segregates to the grain boundaries and increases the risk of hot cracking [7]. The phase diagram of the four component system Ag-Cu-Zn-Si helps to understand the role of silicon. In Figure 3 the influence of the Cu:Zn ratio in 925Ag alloys is shown for silicon free alloys (left diagram) and alloys containing 0,1% silicon (right diagram). The liquidus temperature is practically not affected by the addition of silicon. However, the melting range is largely increased and many different brittle intermetallic compounds form. Zinc promotes the formation of these brittle silicide phases. For alloys with up 2% Zn an 0,1% Si the amount of intermetallic compounds remains relatively small. For this reason higher amounts of Si and Zn should be avoided in 925 silver alloys.

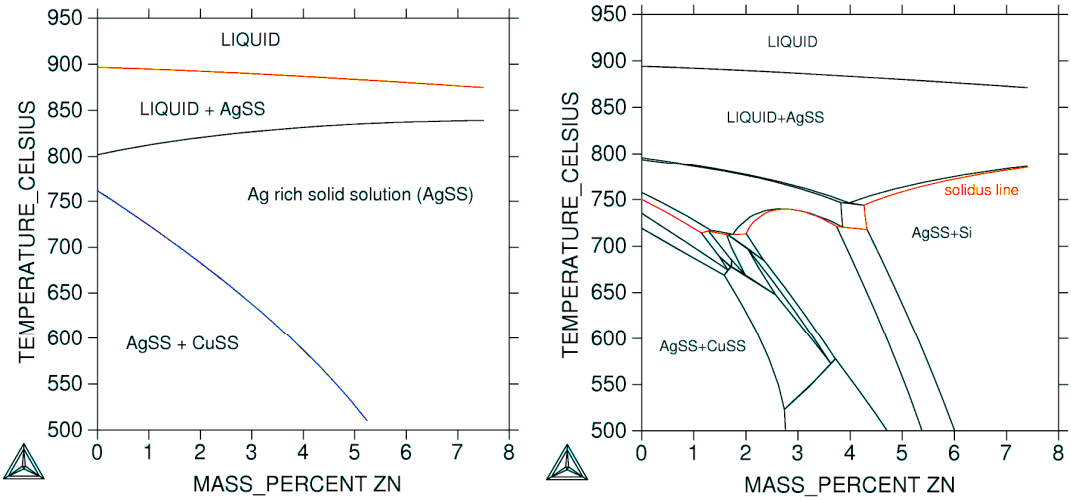

Figure 3: Right: Section through the Ag-Cu-Zn system with a constant content of 925Ag and an exchange of the remaining 75Cu by Zn. Left: Same calculation for an alloy containing 0,1% Si.

1.4 Non equilibrium calculations of 925 silver alloys

In binary Ag-Cu alloys the segregation of Cu is quite strong. This results in the formation of the Ag-Cu eutectic, although is should actually not form according to the equilibrium phase diagram. In order to consider the non-equilibrium cooling the ThermoCalc software allows so-called Scheil-Gulliver calculations. Figure 4 shows such calculations for different alloys with increasing Si content. In the binary Ag-Cu alloy (black curve) the amount of the Ag rich solid phase (AgSS) increases with decreasing temperature until the binary eutectic temperature is reached (horizontal line) and solidification is completed (mole fraction of solid phase = 1). Small additions of silicon dramatically decrease the solidus temperature below 700°C. The minimum values are achieved for 0,1-0,2 % Si. With further increasing Si content the solidus temperature rises again to about 780°C.

This behaviour can be explained by a section through the ternary equilibrium phase diagram Ag-Cu-Zn-Si shown in Figure 3. Small additions of Si result in the formation of different brittle intermetallic compounds which form deep melting eutectics with the AgSS and each other. This explains the extensive lowering of the melting point. In Sterling silver alloys the maximum value of Si is usually restricted to about 0,2%. As the calculations show this results in the lowest solidus temperature and the excessive formation of intermetallic compounds is still avoided.

The addition of zinc reduces the formation of the Ag-Cu eutectic. This practical observation can be confirmed by non-equilibrium calculations (Figure 4, right). The binary Ag-Cu alloys show a eutectic fraction of over 10% (as represented by the horizontal line at 770°C). The replacement of 25Cu by Zn removes the eutectic phase and reduces the solidus temperature by about 100°C. The combined addition zinc and silicon, which is used in commercial alloys, shows a further increase of the melting range of the alloys. The highest reduction is achieved for alloys with a Si content of 0,1%, while alloys with higher Si content show a smaller melting range again. In summary, the non-equilibrium calculations can explain the beneficial casting behaviour of 925Ag-Cu-Zn-Si alloys. They provide a deeper understanding of the role of the different alloying elements and the required amounts in order to achieve optimum processibility.

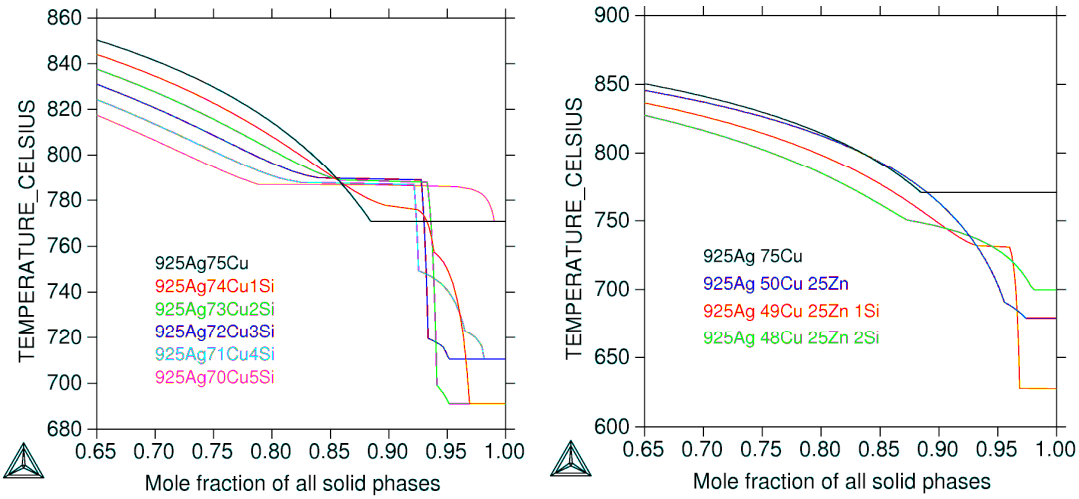

Figure 4: Non equilibrium solidification of 925Ag-Cu-Si alloys with different Si content (left) and 925 Ag-Cu-Zn-Si alloys (right).

1.5 Gold alloys

The main alloying elements in carat gold alloys are Ag, Cu, Zn in yellow and red gold alloys and Ni and/or Pd in white gold alloys. Further alloying elements used in very small additions are deoxidisers (Si, Ge) and grain refiners (Co, PGM). Therefore, usually four component systems have to be considered. In order to present a four component system a four dimensional diagram would be required. Therefore, temperature-concentration sections (so-called isopleths) or projections are used to present the information in two dimensions. Different kinds of sections in a simple ternary system are illustrated in Figure 5. A projection of several of the red isothermal sections at different temperatures to the base provides the liquidus surface of a ternary system.

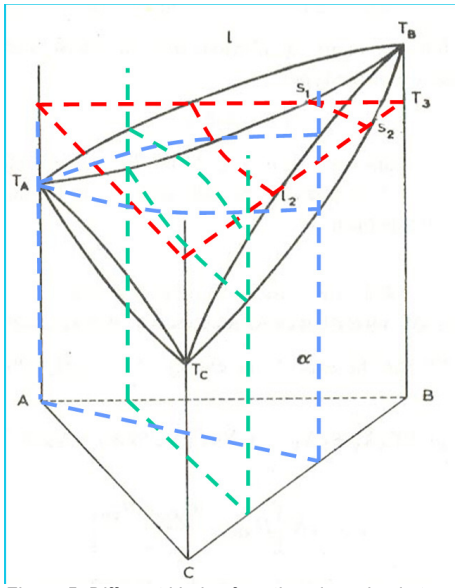

Figure 5: Different kinds of sections in a simple ternary system.

In order to present quaternary systems in a similar way the content of one alloying element (gold) has to be kept constant. In the following the liquidus surfaces of several four component gold alloy systems were calculated and compared with experimental values in order to check the reliability of the used database. A large amount of melting range data of technical alloys were available for comparison from literature [8, 9] or provided by the alloy manufacturers [10, 11]. Some of these alloys contained further alloying elements such as grain refiners (Co, PGM) or deoxidisers (Si, Ge), especially in the case of the 14k alloys. Such alloying additions, which are usually not specified, might influence the melting range of the alloys as described above for Si in silver alloys.
Figure 6 shows the comparison of the calculated liquidus temperature with experimental values for 14 karat yellow and red gold alloys. The gold content is kept constant at 14 or 18 karat and the isothermal liquidus lines

were plotted as function of the Ag and the Zn content. The Cu content of the alloys can be calculated from the difference to 100%. The calculated and the experimental values are in quite good agreement although the experimental values are usually higher than the calculated ones. However, in such comparison it has to be kept in mind that the experimental values also show some scattering, especially when comparing alloys from different sources. The determination of the liquidus temperature is difficult in case of alloys with high zinc content, as zinc evaporates from the alloys during melting. In a subsequent melting experiment the melting point is higher than during initial melting (Figure 7). Taking into account the experimental scatting it can be concluded that the used database provides reliable results for 14k and 18k yellow and red gold alloys.

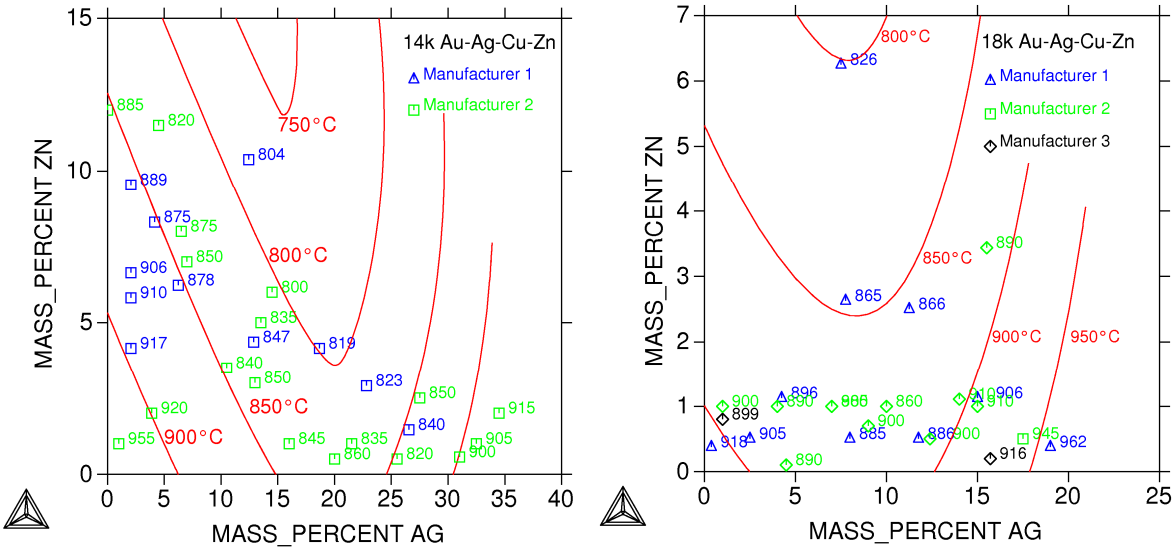

Figure 6: Calculated liquidus surface of Au-Ag-Cu-Zn yellow and red gold alloys compared to experimental datapoints. 14k alloys (left) and 18k alloys (right).

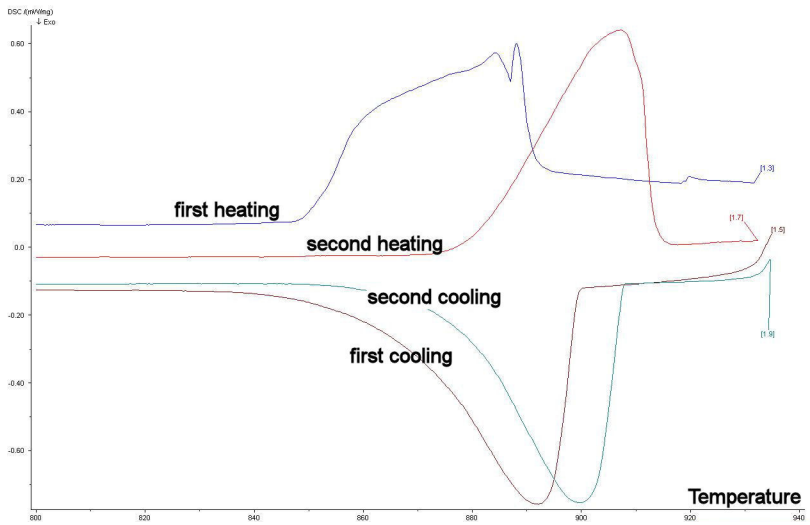

Figure 7: Experimental DTA curves of a 14k yellow gold alloy with about 9% Zn. Due to the evaporation of zinc the solidus and the liquidus temperature of the alloy is 30-40K higher in the second melting run.

The comparison for Ni and Pd white gold alloys is shown in Figure 8 and Figure 9, respectively. Fewer experimental data were available for comparison. For the Ni white gold there is no agreement between calculation and experiment, even when taking into account the experimental uncertainties. The sensitivity of the liquidus curves on the zinc content is much higher than the experimental values. The reason for this discrepancy lies in the poor modelling of the Ni-Zn binary system in the used database. Therefore the database requires improvement in this particular part.

In case of the Pd white gold alloys too few data are available and the composition range of the available alloys is too narrow. Further data from different manufacturers would be required for a reliable comparison. Among the

binary sub-systems of the Au-Ag-Cu-Pd-Zn system the Pd-Zn system is also requiring to be re-assessed and modelled. However, for low zinc contents of 1% the calculated values show a relatively good reliability (Figure 9, right), especially when taking into account the experimental scattering.

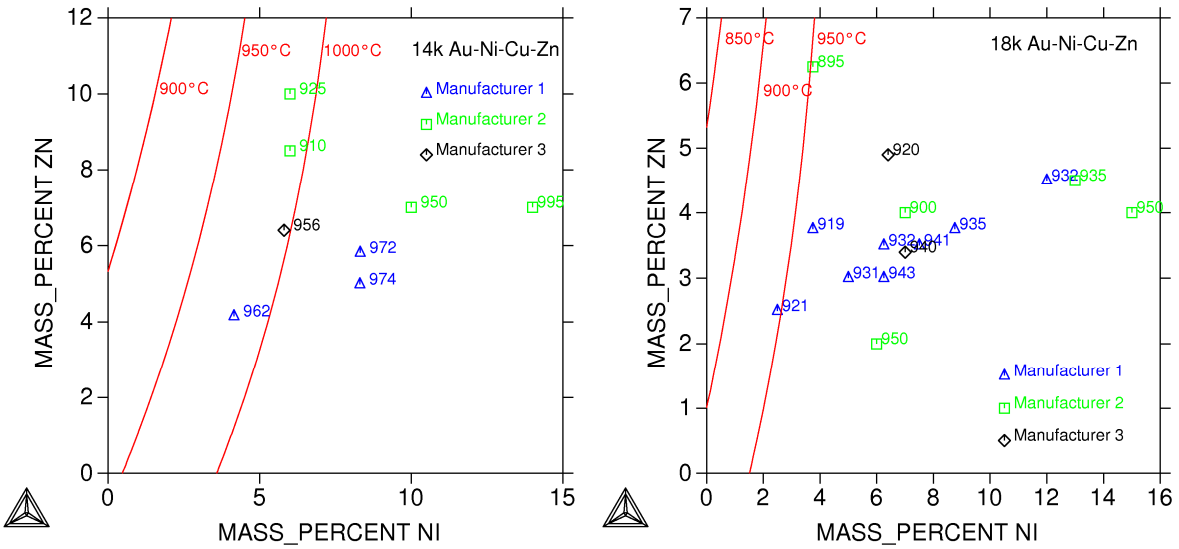

Figure 8: Calculated liquidus surface of Au-Ni-Cu-Zn white gold alloys compared to experimental datapoints. 14k alloys (left) and 18k alloys (right).

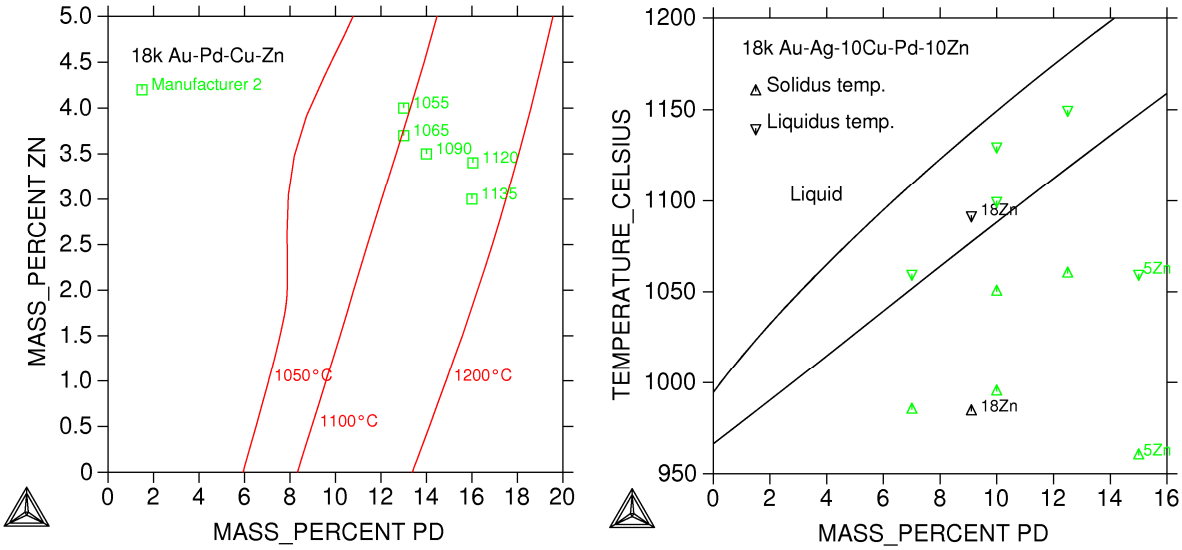

Figure 9: Calculated liquidus surface of 18k Au-Pd-Cu-Zn white gold alloys compared to experimental datapoints (left). Isopleth section through the Au-Ag-Cu-Pd-Zn system for 585Au-10Cu-10Zn. Comparison with experimental solidus and liquidus temperatures (right).

Based on the assessment of the reliability of the used databases different materials properties, such as solidus and liquidus temperature, enthalpy or heat capacity can be easily calculated. Such properties are required during alloy development or for the casting simulation. Figure 10 shows the heat capacity of a typical 18 karat yellow, red and Pd white gold composition. For comparison of the alloys the temperature was normalized with the liquidus temperature. The heat capacity is a measure for the energy released when the temperature is lowered by a certain value. The heat capacity of alloys is nearly constant in the solid and the liquid phase. During phase changes (solidification) the heat capacity increases strongly and reaches a constant value again when the solidification is finished.

A pronounced difference between the alloys is obvious and the effect on the shrinkage porosity will be discussed. Experimentally determined cooling curves from casting experiments reflect the influence of the heat capacity on the thermal response of the system. Cooling curves of different alloys can be found in [12]. During solidification the red gold alloy shows the strongest increase of heat capacity, i.e. a large amount of energy has to be released before the temperature decreases further. This is reflected in a pronounced holding time in the

cooling curve. Once the initial cooling has happened the solidification quickly proceeds. In a casting experiment this results in poor feeding ability in the later stages of solidification and shrinkage porosity in consequence.
The yellow gold alloy shows an increasing heat capacity as the solidification continues. This means more and more energy is released during completion of the solidification and the solidification process will become slower to the end. That allows continuous feeding until the end of the solidification and hence the lowest risk of shrinkage porosity.
The Pd white gold alloy shows the largest melting range, more than three times larger than that of the yellow and the red gold. The heat capacity is relatively low. The temperature will therefore decrease relatively fast and hence solidification. The time for feeding is limited and shrinkage porosity can occur. Thicker sprues or risers can help to slow down solidification and increase the time for feeding of the part.

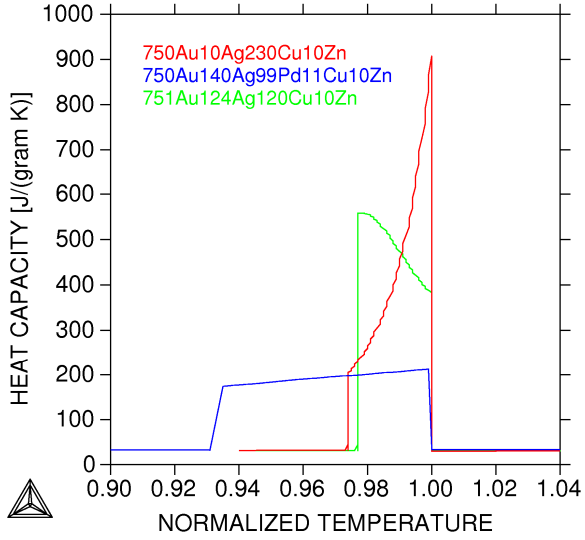

Figure 10: Calculated heat capacity of a typical yellow, red and Pd white gold alloy plotted as a function of the normalized temperature T / TLiquidus.

2 Computational Fluid Dynamics

2.1 State of the art

In this chapter the focus will be on casting simulation, the influence of material's properties and possibilities and limitations of this method. Casting simulation has been applied to precious metal casting processes for a few years now (at least since 2005) [13, 14] and it has proved to be a useful tool in investigating the behaviour both for the metal flow and of the solidification, also for complex parts such as filigree objects [15-17]. The previous research and application of casting software were focused on the static casting process in which the filling of the mould occurs by gravity / applied pressure, and dealt with benchmark casting trials monitored via thermocouples or sensors and the comparison with the simulation output.
The software available on the market allows to model the filling of the mould and the following solidification of the metal providing the user with a prediction on the porosity present in the cast part. The work conducted up to this point indicates a satisfactory comparison between the prediction of the numerical model and the measurements performed during the casting trials both in terms of filling time and of temperatures of the system mould + cast part.

2.2 Possible applications

Casting simulation uses computational fluid dynamics (CFD) to calculate the filling of the mould and the subsequent solidification. The ability of the CFD to predict the flowing of a fluid in a cavity can be exploited to optimize the sprue system of a cast part to reduce turbulence during filling and most of all to insure a proper temperature distribution and a directional solidification, in order to reduce the formation of shrinkage porosity.
The first example in Figure 11 and Figure 12 shows the evaluation of two different kind of feeding possibilities, and the first one, though asymmetrical, seems to provide a more uniform temperature distribution in the part at the end of the filling. The simulation can then be used to identify in advance which geometries could lead to

potential formation of porosity, and which places are more likely to be critical, and used to optimize the sprue system consequently (see Figure 13 and Figure 14).
The heating up of the investment mould right after the casting can also be calculated (Figure 15), and its influence can be taken into account: a very hot mould will facilitate the formation of porosity due to the chemical reaction with the molten metal, but this effect cannot be taken into account by the software, and its influence must be then evaluated according to the operator's experience. This can be generalized to the entire approach that one should have with the simulation in order to apply it in a feasible and efficient way: as a tool able to point out certain problems (wrong feeding system, or mould temperatures for example) which need to be solved according to the operator's experience. In this sense, the CFD can be used as a method to optimize certain aspects of the process, without having the expectation of finding out the exact machine parameters to obtain a porosity free and perfectly filled casting.

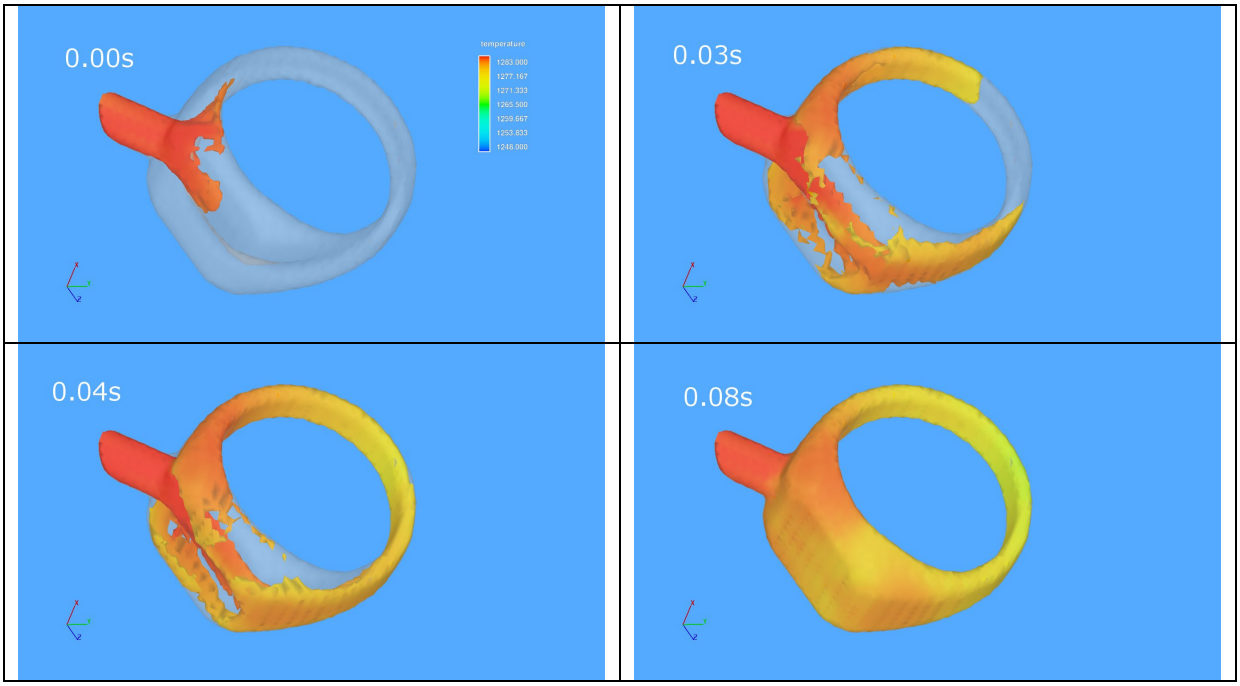

Figure 11 - Example of filling simulation of a ring with feeding sprue on the side

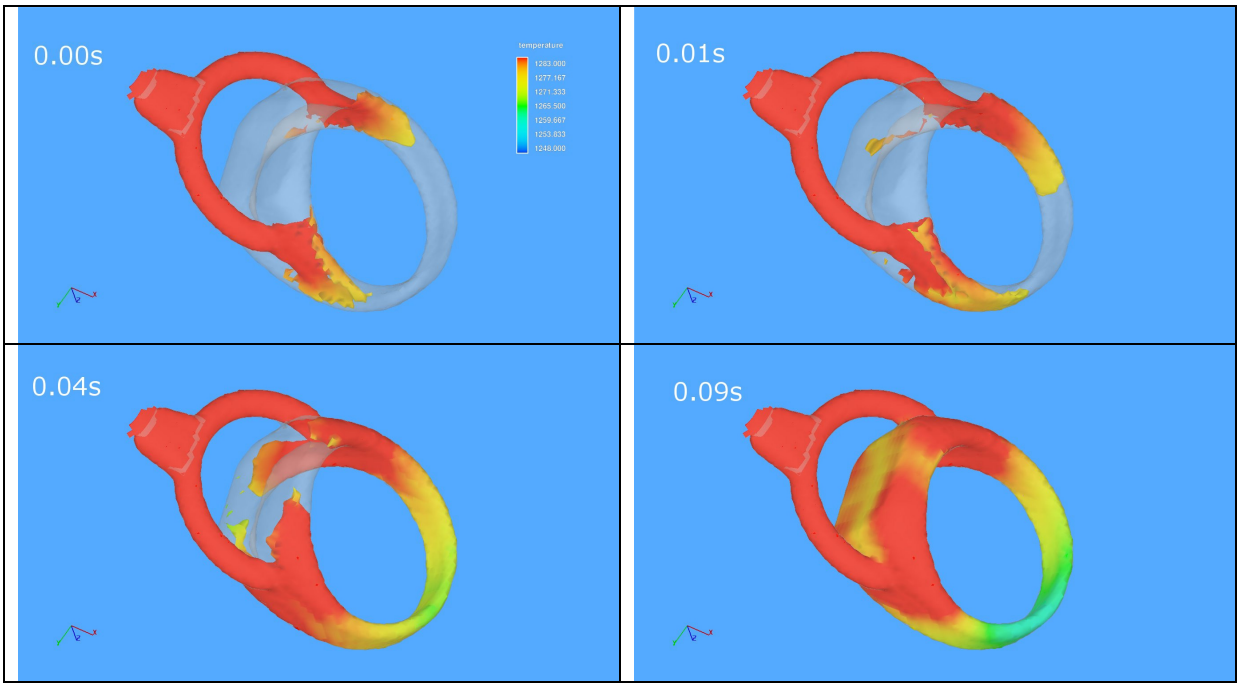

Figure 12 - Example of filling simulation of a ring with symmetrical feeding system

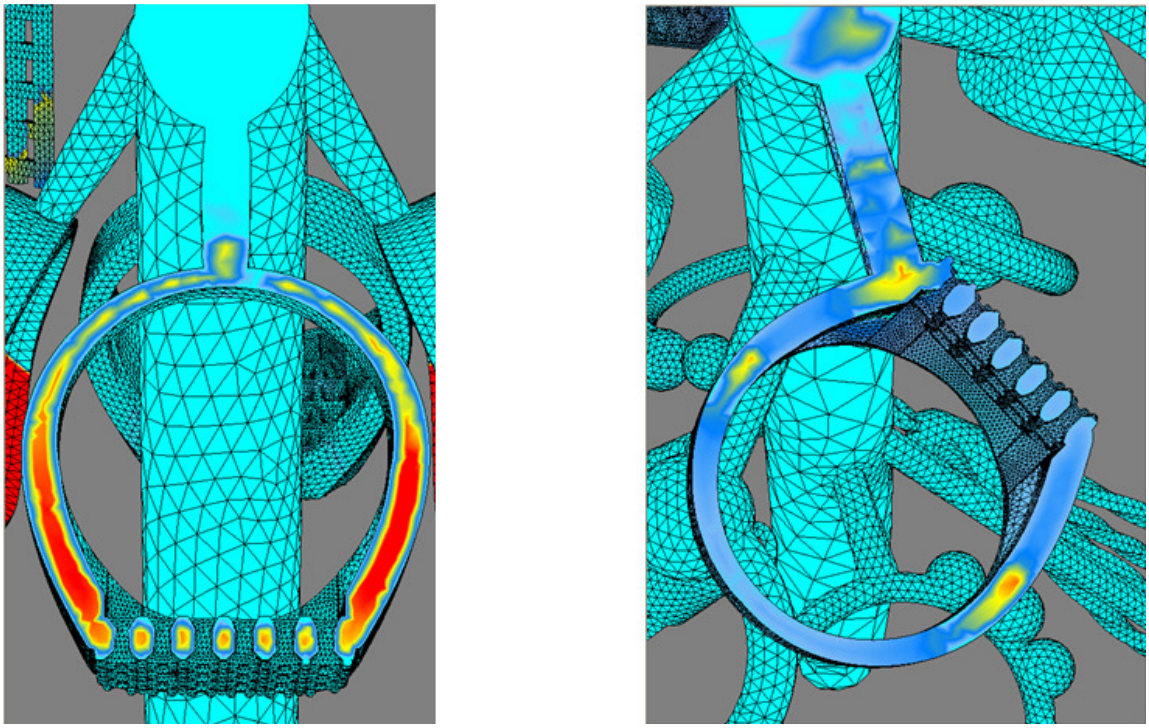

Figure 13 - Example of predicted porosity for two different sprues. Red and yellow colour indicate highest porosity levels.

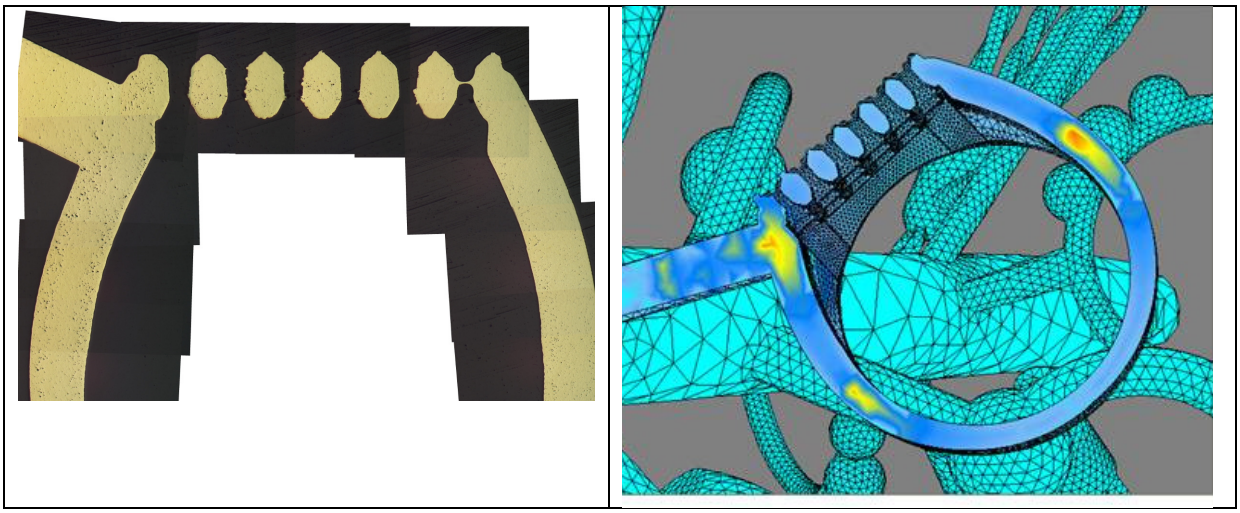

Figure 14 - Example of predicted porosity (right) and matching metallography (left) on the cast part.

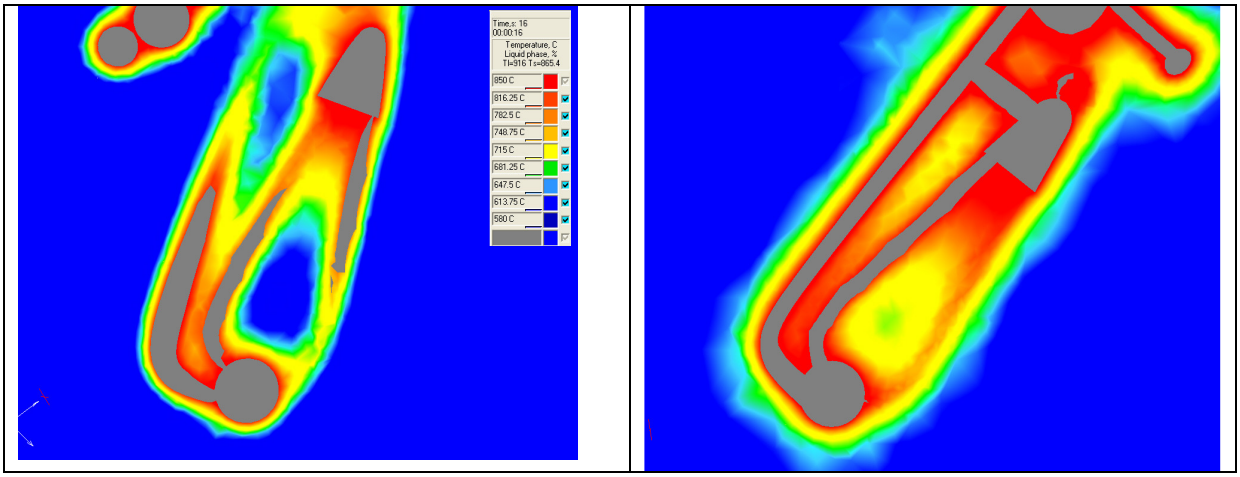

Figure 15 - Example of investment heating with a flask temperature of 500°C (left) and 600°C (right)

2.3 Parametrization

Before being able to run a calculation, it is always necessary to enter the material properties the software needs for the processing: it is in most cases not worth spending weeks in measuring physical properties (such as specific heat, thermal conductivity, etc), which sometimes can be determined only with great difficulty, in order to characterize the materials before the simulation can be finally started: due to the standard response of a specific software (several are available on the market), and (most of all) to the fit parameters that need to be adjusted to approach to the experimental results, the influence that the material properties have is always mediated.
In a previous research project, it was observed how a variation of the thermal conductivity in the alloy (in the range of 5-10 %) didn't have a considerable influence on the cooling curves obtained in the simulation (see Figure 16): this can be considered on one side as a lack of sensitivity of the software to the alloy properties, but on the other side it allows the operator to start the calculation with the eventual data set already available avoiding spending too much time in the material characterisation phase; an eventual refining of the material parametrization could be eventually performed later, if necessary.
Another interesting example that highlights the influence of material parameters was conducted by taking two very different thermal conductivities to calculate the cooling of a part: one measured for the specific alloy in question (a 14kt WG), and one "adapted" (based on the experience acquired on previous trials on 18kt YG). The matching of the software with the thermocouple curves is slightly improved (Figure 17 and Figure 18). The new thermal conductivity offers a better match for the undercooling, but the effect on the general cooling is relatively small despite the two very different set of alloy data, which proves the importance and the influence of the internal fit parameters over the end result: these parameters regulate the heat transfer between the metal and the mould, they are present in every software package and they have a predominant position in the fine tuning of the calculation and they should be optimized with benchmark trials when possible. The different software available on the market uses different strategies to balance between the influence of material properties and fit parameters, respectively. The bottom line is that having a perfect set of material data does not assure a corresponding matching on the output side, which forces the user to accept a compromise on the precision of the obtained results, or as an alternative to perform a series of time consuming adjustment on the software parameters. Future development of the software and hardware will allow relying more on physics-based models rather than on fit parameters.

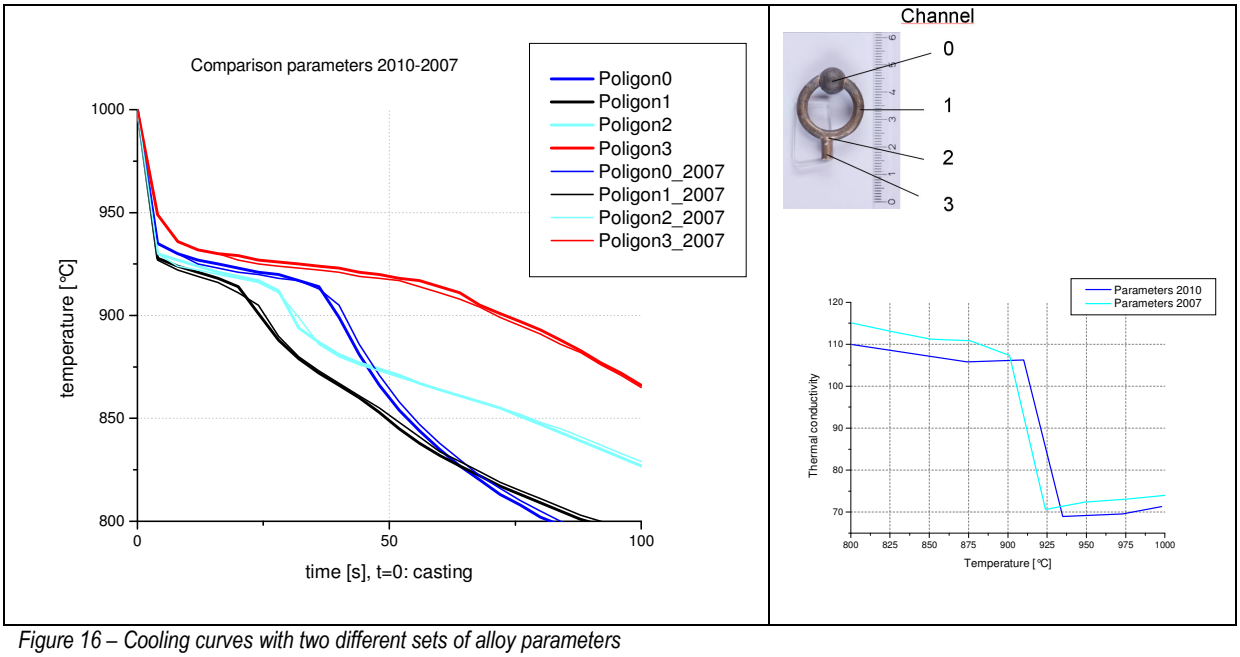

Figure 16 – Cooling curves with two different sets of alloy parameters

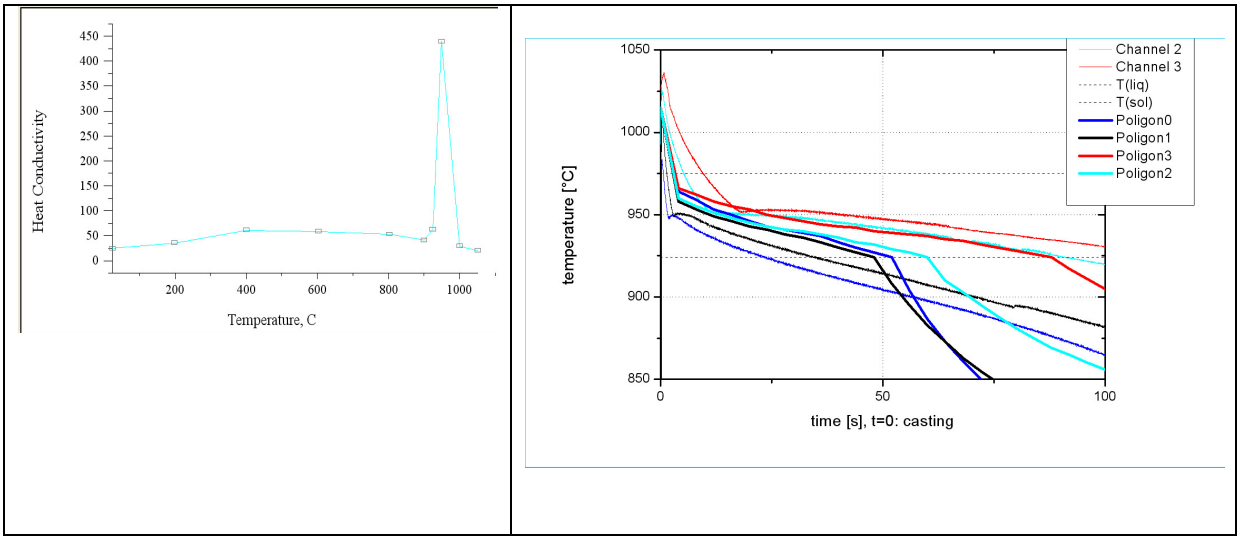

Figure 17 - Measured thermal conductivity for a 14kt YG, and corresponding matching with the experimental cooling curves

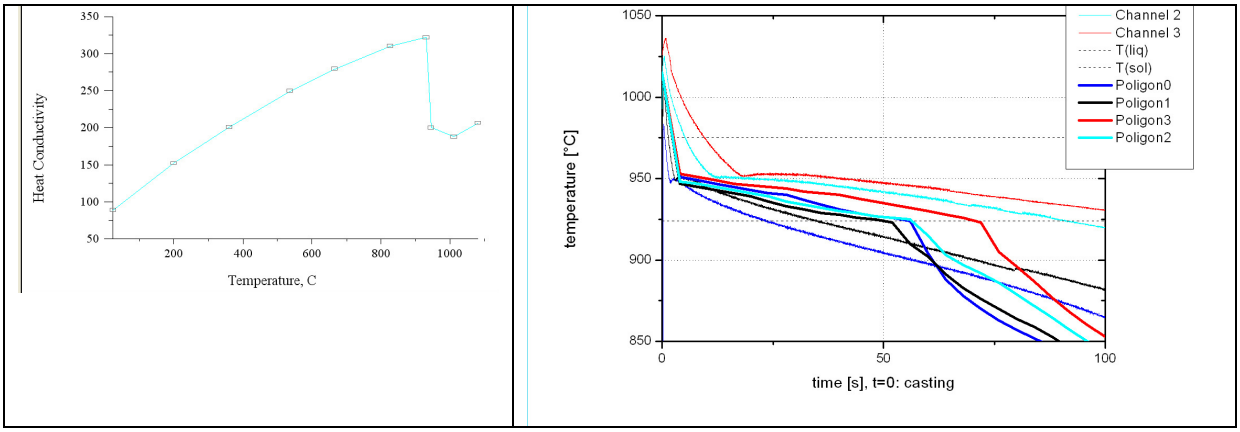

Figure 18 - Adapted thermal conductivity, and corresponding matching with the experimental cooling curves

2.4 Limitations

When one approaches the simulation and its application to practical cases, it must not be expected to be able to "predict" the result of a casting, or to set-up the casting machine to obtain the best possible result in terms of "porosity free parts". The investment casting procedure is influenced by several factors: performance of the refractory material (which can vary from batch to batch), chemical reaction between the hot metal and the mould, the influence of the furnace during the burn-out of the flask is relevant e.g. two flasks prepared in two different ovens can have a significantly different performance. All these aspects cannot be taken into account in the simulation, and therefore it is better to know how to employ it in a meaningful way: for example being able to evaluate the effect of the mould temperature (as in the example shown in Figure 15) and the possible influence on the investment reaction that could lead to gas porosity.

Moreover, it must be considered that CFD requires a certain amount of time to provide a result, and in many cases it cannot be used as "an emergency" solution to an urgent production problem. The time necessary to process the geometry files, perform the meshing and wait for the calculation to complete is unfortunately much superior to the one necessary to run a "quick" experimental trial, not considering the fact that the output necessitates to be evaluated by an experienced person. Perhaps in the future the speed of the calculation will increase, allowing for quicker trials, and reaching a comparable time with the experimental counterpart.

In other industrial sectors the cost of the moulds are much higher, the pieces are produced in a larger number, and the possibility of saving money and testing different solutions before moving to the production phase is at hand and more concrete. The application of CFD is therefore more suitable to assist in the design phase of the parts, in order to establish the better position, shape and diameter of the feeding system according to the turbulence observed during the filling, and having therefore the chance of intervene "before" the production

starts. Otherwise then the re-design of the sprue is not economically feasible anymore, and the only parameters left to change in order to solve a filling or porosity issue are the metal or the mould temperatures.
The adjustment and refinement of the results through the software parameterization is possible when a series of experiments with thermocouples and metallographical investigations have been run in advance, and can offer a basis for benchmarking. In "normal" cases (to approach an industrial everyday situation) the background work of benchmarking tests is not always available, and thinking of optimizing the software for every different alloy and investment (which has a great influence on the heat transfer and therefore on the cooling of the metal) is obviously not possible, both for time and costs reasons.

2.5 Further applications

Further applications, which are currently being tested and will be applied in a future research project, are the centrifugal and the tilting casting processes. The CFD can be applied to the centrifugal process to establish how the centrifugation influences the filling of the parts according to their positioning, or to the type of adopted main sprue (Figure 19).
The simulation can be also applied to the tilting process, and first tests have been focused on the rotation angle and the speed of rotation, and how these parameters condition the flowing of the metal out of the crucible (Figure 20). Different crucible geometries could also be tested to choose the best one for the pouring of the metal. For instance such tests could be used during the machine development to achieve a proper design of the tilt mechanism and the machine geometry.
A further example is shown in Figure 21 where a simple form with a plate was filled with 18kt YG alloy in order to evaluate the influence of the cooling speed on the solidification. A comparison with metallography (Figure 22 shows a good matching with the simulated turbulences and the resulting solidification profile in the metal; this case shows the potential of the CFD to predict the effect of the turbulences during the pouring of the melt in tilt casting. Potential applications for precious metal industry lie in the tilt casting of semi-finished products, such as bars, in order to avoid the formation of shrinkage porosity, which cause the rejection of part of the casting (with the resulting cost). By acting on critical parameters such as the cooling of the mould or the diameter of the bar it can be virtually evaluated how they interact with each other in order to obtain a directional solidification.

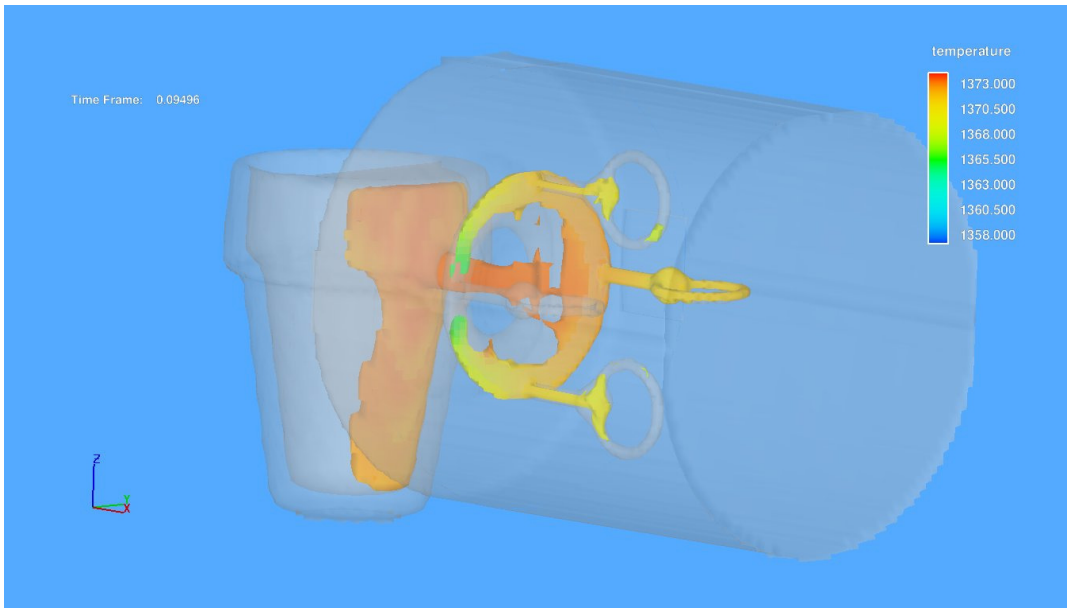

Figure 19 - Example of centrifugal casting simulation with temperature distribution

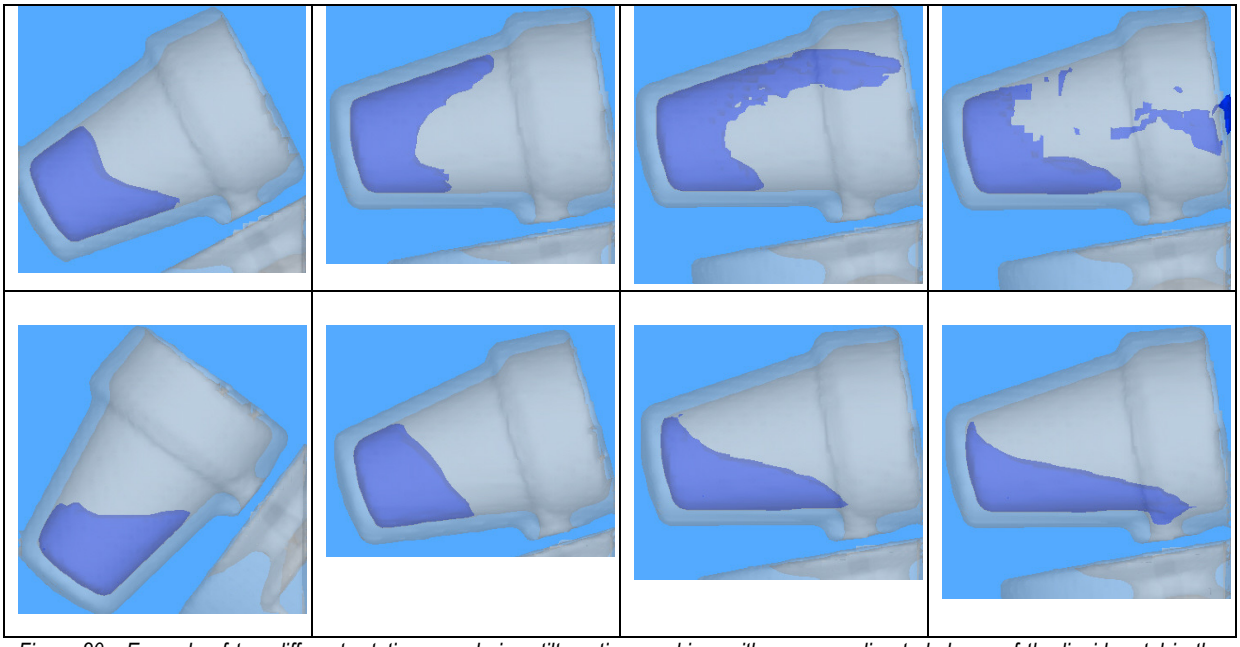

Figure 20 - Example of two different rotation speeds in a tilt casting machine, with corresponding turbulence of the liquid metal in the crucible

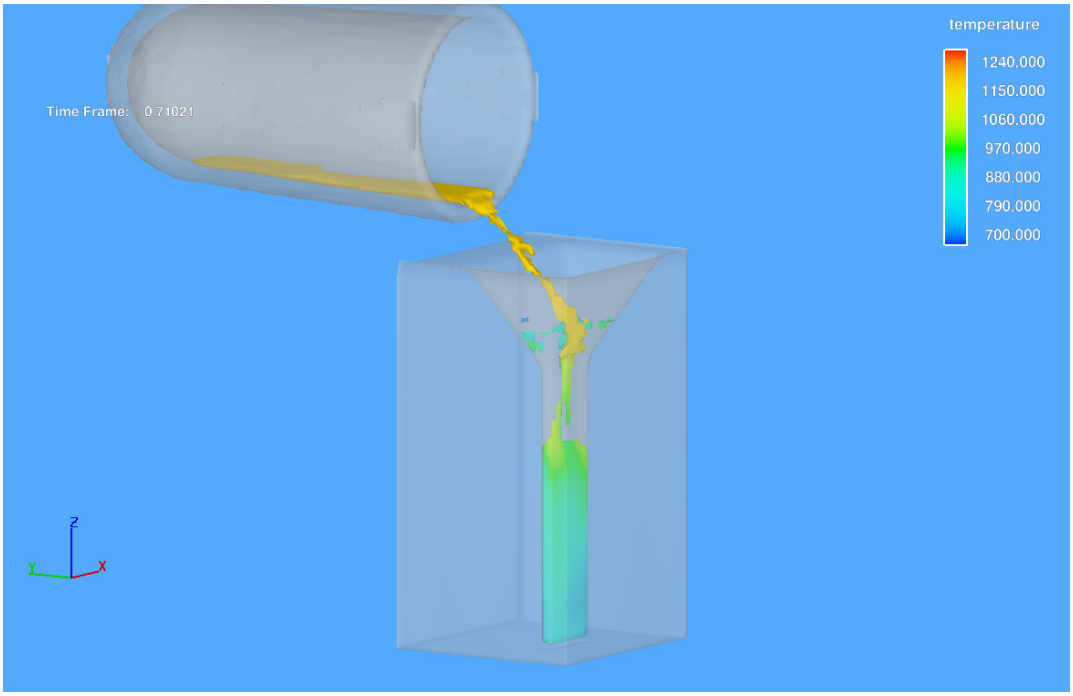

Figure 21 - Example of tilt casting

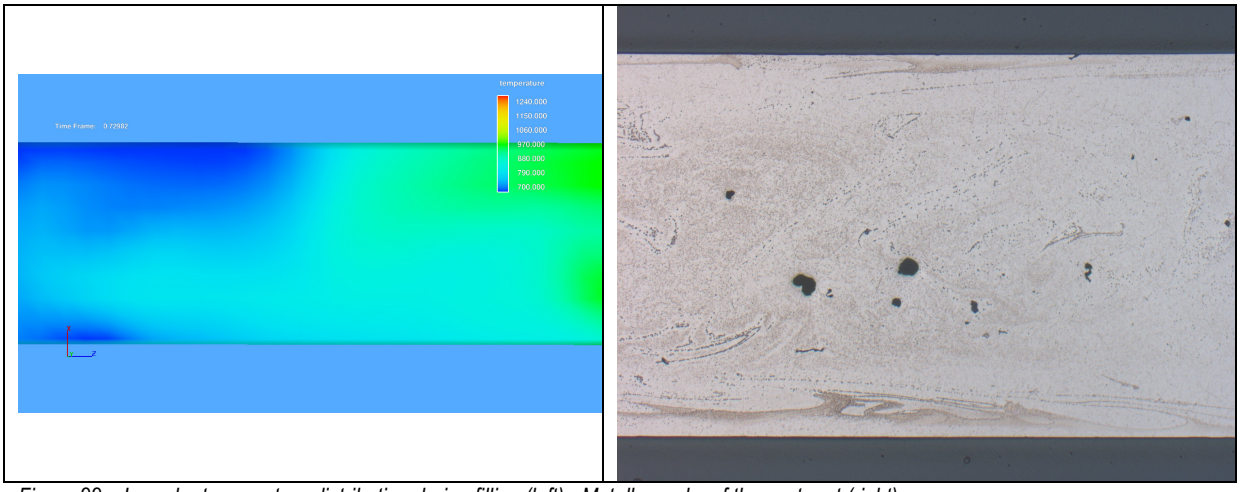

Figure 22 – Irregular temperature distribution during filling (left) - Metallography of the cast part (right)

3 Summary and Outlook

In many industry sectors thermodynamic simulation has been proofed as a useful tool in alloy development and in the understanding of material and processing problems. So far, in the precious metals industry such simulation has been rarely applied. The thermodynamic databases, which are available commercially for precious metals, are reliable for the calculation of equilibrium and non-equilibrium phase diagrams of Sterling silver, yellow/red gold alloys and Pd white gold alloys, especially for those with low zinc content. With the current databases the reliable simulation of Ni white gold alloys is not possible, because the binary Ni-Zn system is modelled insufficiently and needs to be re-assessed. Further development of the databases is therefore necessary to widen the application of thermodynamic modelling.

Such application could be in the determination of materials properties for casting simulation. As all casting simulation software still require some fit parameters to obtain good results, it might not be necessary to determine material parameters of highest precision. Instead a set of meaningful parameters determined by thermodynamic simulation is sufficient to obtain reasonable casting simulation results. Casting simulation requires a time consuming modelling and meshing of the parts to be simulated. It should therefore not be considered as a tool to solve problems in daily casting practice with many changing parameters. Instead, it can be used successfully to develop design strategies e.g. for sprue sizes and geometries or to study the principle influence of the process parameters in investment casting. A very interesting application of casting simulation lies in the design and engineering of tilt and centrifugal casting machines and processes.

Further development of simulation software (both for casting and for thermodynamics) and databases will be required in future. A limited number of meaningful experiments with known experimental error will always be required for correlation of simulation. By taking into account the limitations of the simulation complex multi-parameter problems can be solved by the experienced operator of the software.

Acknowledgements

The European Commission is acknowledged for financial support of this study under the contract no. 222179-INTOGOLD. The authors thank the partners of the INTOGOLD project for the good co-operations, the provision of materials and the many fruitful discussions. Special thanks are to the members of the metallurgy department of FEM, namely Franz Held and Ulrike Schindler, for their commitment to the INTOGOLD project. Mr. Thomas Laag from C. Hafner (Pforzheim, Germany) and Mr. Jörg Fischer-Bühner (Legor, Italy) are acknowledged for providing melting range data of numerous alloys.

References

1. Chang, Y.A., *Phase diagram calculations in teaching, research and industry.* Metallurgical and Materials Transactions B, 2006. **37**(1): p. 7-39.
2. Massalski, T.B., *Binary alloy phase diagrams*. Vol. 1+2. 1986, Metals Park, Ohio: American Society of Metals.
3. Okamoto, H. and T.B. Massalaski, eds. *Phase diagrams of binary gold alloys*. 1987, ASM International, Metals Park, Ohio, USA.
4. Prince, A., G.V. Raynor, and D.S. Evans, *Phase diagrams of ternary gold alloys*. 1990, London: The Institute of Metals.
5. Saunders, N. and P. Miodownik, *CALPHAD: a comprehensive guide*, ed. R.W. Cahn. 1998, New York: Elsevier.
6. Lukas, H.L., S.G. Fries, and B. Sundman, *Computational Thermodynamics, The CALPHAD Method*. 2007, Cambridge UK: Cambridge University Press.
7. Fischer-Bühner, J. and R. Bertoncello. *Silver casting revisted: the alloy perspective*. in *The Santa Fe Symposium*. 2010. Albuquerque, NM, USA: Met-Chem Research.
8. Di Siro, M., et al. *Characterization of 9, 10, 14 and 18 Karat gold alloys*. in *The Santa Fe Symposium*. 2010. Albuquerque, NM, USA: Met-Chem Research.
9. Maggian, D., S. Bortolamei, and M. di Siro. *Characterisation of 14-Karat gold alloys*. in *The Santa Fe Symposium*. 2011. Albuquerque, NM, USA: Met-Chem Research.
10. Laag, T., *Melting range of 14 and 18 karat gold alloys of C. Hafner GmbH+Co. KG, Pforzheim, Germany.* personal communication, 2011.
11. Fischer-Bühner, J., *Melting range of 14 and 18 karat gold alloys of Legor Group Srl, Bressanvido, Italy.* personal communication, 2011.
12. Fischer-Bühner, J., *Advances in the prevention of investment casting defects assisted by computer simulation*, in *The Santa Fe Symposium on Jewelry Manufacturing Technology*, E. Bell, Editor. 2007: Albuquerque, NM, USA. p. 149-172.
13. Actis-Grande, M., et al., *Computer simulation of the investment casting process: experimental validation*, in *TCN CAE Conference*. 2005: Lecce, Italy. p. 63-73.
14. Actis-Grande, M., et al. *Computer simulation of the Investment casting process:Experimental validation*. in *4th International Jewelry Symposium*. 2006. Saint Petersburg, Russia.
15. Fischer-Bühner, J. *Computer simulation of jewelry investment casting*. in *The Santa Fe Symposium on Jewelry Manufacturing Technology*. 2006. Albuquerque, NM, USA.
16. Fischer-Bühner, J., *Computer simulation of jewellery investment casting*, in *JTF - Jewellery Technology Forum*. 2006: Vicenza, Italy. p. 241-259.
17. Actis-Grande, M., L. Porta, and D. Tiberto, *Computer simulation of the investment casting proess: widening of the filling step*, in *The Santa Fe Symposium on Jewelry Manufacturing Technology*, E. Bell, Editor. 2007: Albuquerque, NM, USA. p. 1-18.